Jurnal Pendidikan Teknologi Kejuruan, Vol. 7, No. 2, pp. 115-125, May 2024
e-ISSN 2621-1548; p-ISSN 2621-3273

Enhancing biodegradable polymer surface wettability properties through atmospheric plasma treatmsurfaent and nanocellulose incorporation

Shih-Chen Shi[1*], Chia-Feng Hsieh[1] and Dieter Rahmadiawan[1,2]

[1] Department of Mechanical Engineering, National Cheng Kung University, **Taiwan**
[2] Department of Mechanical Engineering, Universitas Negeri Padang, **Indonesia**

*Corresponding Author: scshi@mail.ncku.edu.tw
Received March 05th 2024; Revised May 24th 2024; Accepted May 27th 2024

Cite this https://doi.org/10.24036/jptk.v7i2.36723

Abstract: This study investigates the effects of atmospheric plasma treatment on the surface properties of polylactic acid (PLA)/nanocrystalline cellulose (CNC) composites, aiming to improve their wettability and mechanical properties. The research utilizes a twin-screw extrusion process for fabricating PLA/CNC biocomposites, followed by surface modification using a custom-built, with a tenfold high-voltage atmospheric plasma system. The motivation of this treatment was to improved surface wettability and potential for enhanced adhesive bonding in ecological applications. These findings contribute to developing more sustainable composite materials by providing a method to improve the functionality of biodegradable polymers without compromising their environmental benefits.

Keywords: Biodegradable polymers; Polylactic acid; Nanocrystalline cellulose; Atmospheric plasma treatment; Surface wettability

1. Introduction

Plastic deposition in oceans remains a pressing global concern, with millions of tons being introduced annually (*Plastics in the Ocean - Ocean Conservancy*, n.d.). This influx encompasses diverse sources, from urban litter like stray plastic bags and straws to substantial volumes of mismanaged plastic waste from burgeoning economies. Such extensive plastic accumulation profoundly impacts marine ecosystems. Biodegradable materials refer to high polymers capable of undergoing degradation through the action of microorganisms in the natural environment. These polymers maintain good performance during use and, upon disposal, do not pose environmental hazards; instead, they are broken down or digested by natural microorganisms, yielding carbon dioxide and water (Akbar et al., 2024; Makruf et al., 2024; Nurdin et al., 2023; Oktaviani et al., 2023). The literature distinguishes between two concepts: biobased polymers and biodegradable polymers. From a raw material perspective, polymers derived from biomass are termed biobased polymers, contrasting with those derived from petroleum resources, termed petro-based polymers. From a material property perspective, polymers that can decompose by microorganisms are referred to as biodegradable polymers, in contrast to non-biodegradable polymers. Common biodegradable polymers include cellulose (Rahmadiawan & Shi, 2024; Shi et al., 2020; Shi & Huang, 2018; Shi & Wu, 2018), chitosan (Shi, Lu, et al., 2024; Shi & Chang, 2022), and polylactic acid (PLA) (Chou et al., 2021, 2023; Rahmadiawan, Abral, Ilham, et al., 2023; Rahmadiawan, Abral, Shi, et al., 2023).

Extensive research has been conducted on nanocellulose derived from natural sources to enhance

biodegradable polymers' mechanical and tribological properties (Shi, Tsai, et al., 2024; Shi & Tsai, 2022). Cellulose, the world's most abundant renewable resource, boasts an annual production of 830 million metric tons via photosynthesis. This surge in research is propelled by various factors, including concerns over fossil fuel scarcity, escalating costs, heightened environmental consciousness, and burgeoning green energy (Rahmadiawan et al., 2024; Shi, Ouyang, et al., 2024; Shi & Chen, 2023). Meanwhile, the application scope of PLA has continued to evolve since its inception in the early 1980s, initially targeting human organ repair materials like surgical sutures and tissue engineering scaffolds (Agrawal & Ray, 2001). With the rising environmental awareness, the second generation of PLA emerged in the early 2000s, aiming to supplant conventional plastics in short-term-use items and disposable packaging applications.

Recent advancements in nanotechnology and surface engineering have presented potential solutions to these challenges (Koizhanova et al., 2023). Nanocellulose, derived from the abundant natural polymer cellulose, has been explored extensively for its capacity to enhance the mechanical and tribological properties of biodegradable polymers. Furthermore, the application of atmospheric plasma treatments has been identified as a promising approach to modify and improve the surface characteristics of these materials, notably their wettability. Such treatments can alter the surface energy of biodegradable polymers, thereby improving their adhesion properties—a critical factor in many industrial and biomedical applications.

The American Society for Testing and Materials (ASTM) defines substances capable of bonding various materials together, whether similar or dissimilar, by utilizing adhesion to surfaces as adhesives. Adhesives undergo three stages during the bonding process: liquid (adhesive), wetting (on the adherend surface), and curing (adhesive layer). The wettability of material surfaces involves the chemical and physical properties of the interface, determining the ultimate strength of adhesion. Wettability is of paramount importance in adhesive engineering. The paper hypothesizes that atmospheric plasma may cause surface damage, affecting surface roughness. When adhesives adhere to a surface, mechanical interlocking enhances the shear strength of the adhesive (Jordá-Vilaplana et al., 2015; Prolongo et al., 2010).

2. Material and Methods

Polylactic acid (PLA) is a renewable thermoplastic aliphatic polyester derived from sources such as corn starch. This research employed extrusion-grade PLA polymer (Ingeo™ biopolymer 2003D from NatureWorks LLC). Nanocrystalline celluloses (CNCs) are rod-like or whisker-shaped particles obtained via the acid hydrolysis of materials like wheat flour, pea starch, and various cellulose forms. CNC powder, supplied by CelluForce (product name: CelluForce NCC™), was utilized to augment PLA's mechanical properties and thermal stability. The nanocrystalline cellulose (CNC) / polylactic acid (PLA) biocomposite material was synthesized through twin-screw extrusion. Post-extrusion test specimens were fabricated via injection molding following ASTM standards. The atmospheric plasma equipment utilized in this study consisted of a laboratory-designed and assembled jet-type low-temperature atmospheric plasma system. The power supply comprised a high-voltage alternating current power source custom-made by Taiwan Plasma Corporation, amplified tenfold by a high-voltage coil (input voltage: 220 V/60 Hz, output voltage: 1 kV10 kV/1 kHz10 kHz).

The plasma nozzle was also mounted on a three-axis linear stage, with movement paths programmed using MaterCAM to achieve standard numerical control. The nozzle material was polytetrafluoroethylene (PTFE), with an internal electrode consisting of a 1.6 mm copper tungsten electrode needle. Parallel airflow was introduced through a 4 l/min supply of high-

purity argon gas while an alternating current voltage of 8 kV/10 kHz was applied. Finally, a stable plasma jet was emitted from a 2.8 mm inner diameter quartz tube, with a distance of 15 mm between the copper tungsten electrode and the ground electrode.

The surface morphology after atmospheric plasma treatment was measured using a Laser Scanning Confocal Microscope (VK9700, Keyence, Osaka, Japan), and measurement results for surface properties such as Ra, Rq, Rsk, and Rku were obtained using VK-viewer. A cutoff value of 0.8 mm was employed to ensure that the Ra falls within the standard range.

3. Results and discussion

Surface morphology after atmospheric plasma treatment

The 2D roughness profiles of PLA/CNC surfaces before and after plasma treatment were measured using 3D laser scanning, as shown in Figures 1 and 2. Since the mold undergoes polishing before injection molding, the cutoff value should be selected as 0.8 mm, ensuring that the final surface roughness falls within the standard range. Table 1 indicates that there is not much difference in surface roughness parameters between pure PLA and PLA with 1, 3, and 5 wt.% CNC. Even if the Ra values in the parameters are the same, it does not mean that the surface shapes are identical. Therefore, further investigation and quantification of the comprehensive surface parameters Rsk and Rku changes due to plasma etching were conducted.

Table 1 shows positive Rsk values before plasma treatment, indicating that the surfaces primarily comprise peaks. From the 2D roughness profiles in Figure 1, it can be observed that the ratio of roughness peaks to valleys is smaller, and Rku is greater than 3, indicating a peaked shape of the rough curves. The surface morphology parameters after plasma treatment at a nozzle distance of 12 mm from the specimen are listed in Table 2. Although Ra shows no significant change, Rp and Rv are influenced by plasma micro-etching. Compared to Figure 1, Figure 2 shows no apparent peaks on the surface because when free electrons bombard the polymer surface, they erode the peaks on the surface, leaving only valleys. From this surface morphology perspective, the Rsk values after plasma treatment all decrease, even becoming negative for 1~5 wt.%, indicating that the peaks on the surface are removed or deep valleys are generated. Additionally, the values of Rku decrease due to the influence of plasma micro-etching, resulting in a surface with multiple low peaks and small deep valleys.

The surface after plasma treatment exhibits excellent wetting effects primarily due to changes in surface morphology, enhancing the mechanical anchoring effect of the liquid. Secondly, this is attributed to the contribution of hydrophilic functional groups generated on the surface.

Table 1. Surface roughness result for untreated surface

(μm) / Sample	Amplitude Parameters					Comprehensive Parameters	
	R_p	R_v	R_z	R_a	R_q	R_{sk}	R_{ku}
Pure	8.45	3.19	11.64	0.45	0.64	2.55	26.5
1wt%	5.06	4.91	9.97	0.35	0.45	0.24	16.2
3wt%	7.84	7.35	15.20	0.61	0.84	0.99	17.3
5wt%	2.84	7.20	10.04	0.25	0.35	1.84	19.9
Average	**6.05**	**5.60**	**11.71**	**0.41**	**0.57**		

Table 2. Surface roughness results for plasma-treated surface

(μm) / Sample	Amplitude Parameters					Comprehensive Parameters	
	R_p	R_v	R_z	R_a	R_q	R_{sk}	R_{ku}
Pure	7.51	3.08	10.59	0.39	0.52	1.30	14.8
1wt%	7.50	14.4	21.93	0.38	0.51	-0.20	14.1
3wt%	3.28	7.86	11.15	0.43	0.56	-0.70	8.26
5wt%	4.10	9.94	14.04	0.69	0.93	-1.01	8.21
Average	**5.60**	**8.83**	**14.43**	**0.47**	**0.63**		

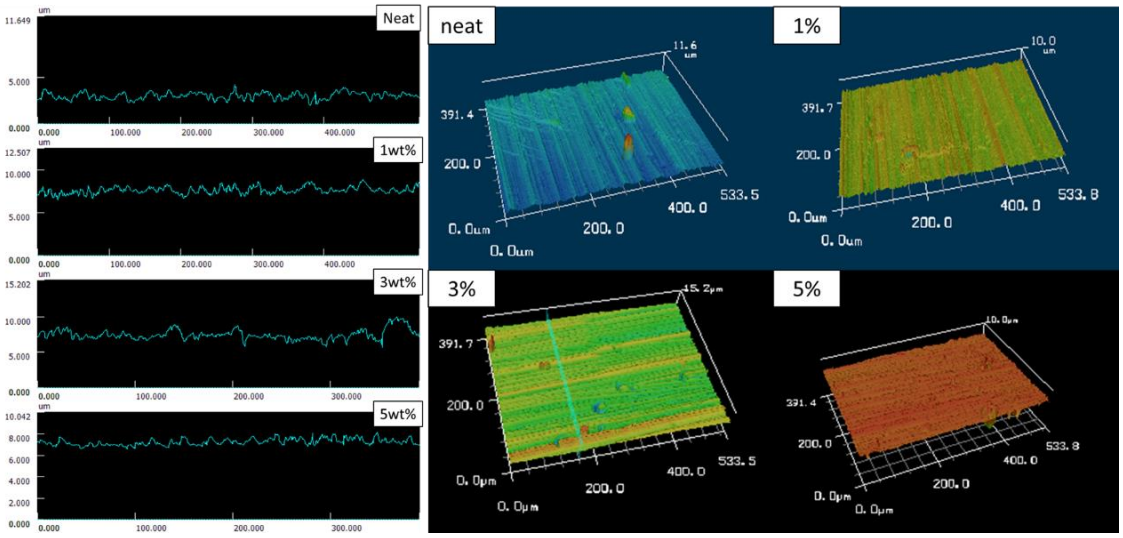

Figure 1. 2D surface roughness profiles and 3D surface topography of untreated surface

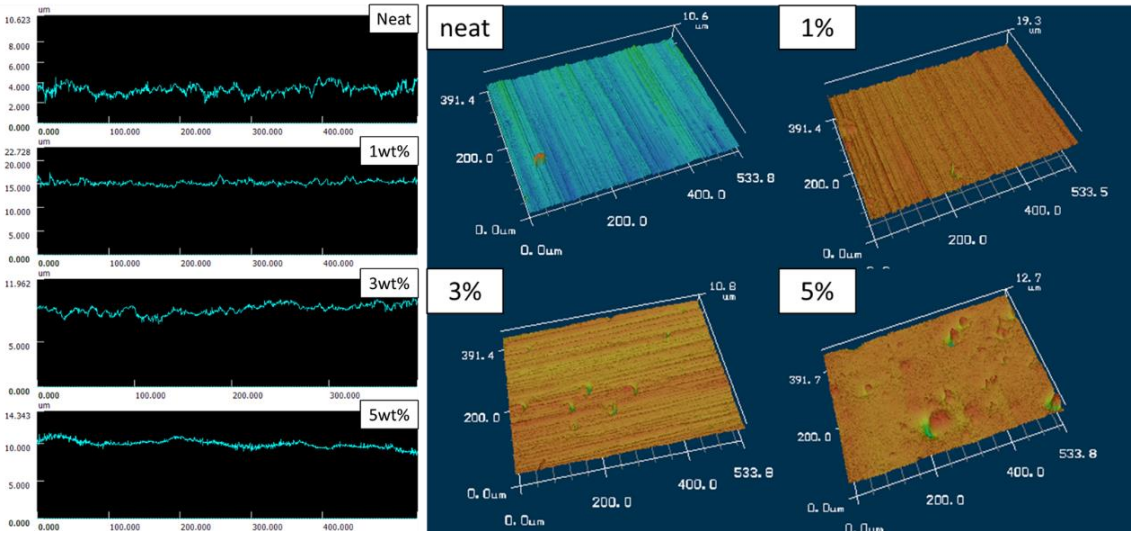

Figure 2. 2D surface roughness profiles and 3D surface topography of the plasma-treated surface

CNC Influence on the Surface Free Energy of PLA

Pure PLA contains polar groups in its main chain, making it partially hydrophilic. However, its

hydrophilicity is relatively low, with an average water contact angle of 64.2° before plasma modification. With the addition of CNC, the contact angle of PLA/CNC decreases slightly compared to pure PLA. This phenomenon is mainly attributed to the presence of hydroxyl groups on the surface of CNC, which is expected to improve the wetting properties of PLA. Consequently, PLA/CNC composite materials exhibit higher hydrophilic characteristics on the surface, thus enhancing the hydrophilic effect of the samples. However, when the content reaches 5 wt.% CNC, the contact angle increases to 64.7°, as shown in Figure 3. This may be due to the aggregation of CNC within the PLA.

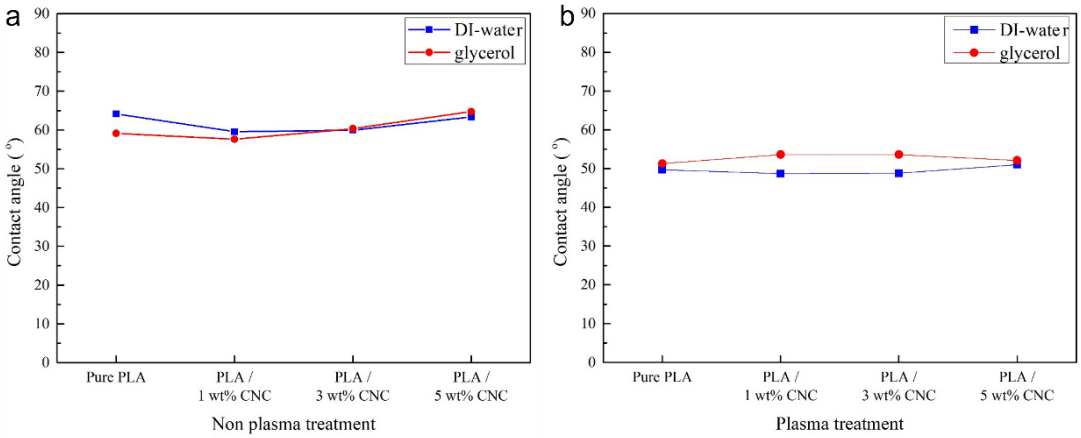

Figure 3. Contact angles of various contents (a) before and (b) after plasma modification

The polar and non-polar contributions to the surface free energy were calculated using the Owens-Wendt equation, and the measurement results are listed in Tables 3 to 6. The average surface free energy is approximately 37.2 mJ/m^2, and there is no significant change in surface free energy due to the introduction of CNC. However, it can be confirmed that the polar interaction force increases with CNC content, reaching a maximum value of 30 mJ/m^2 at 3 wt% CNC. The surface free energy decreases to 27.5 mJ/m^2 when the CNC content reaches 5 wt.%, further confirming that excessive CNC aggregation leads to a decrease in surface free energy.

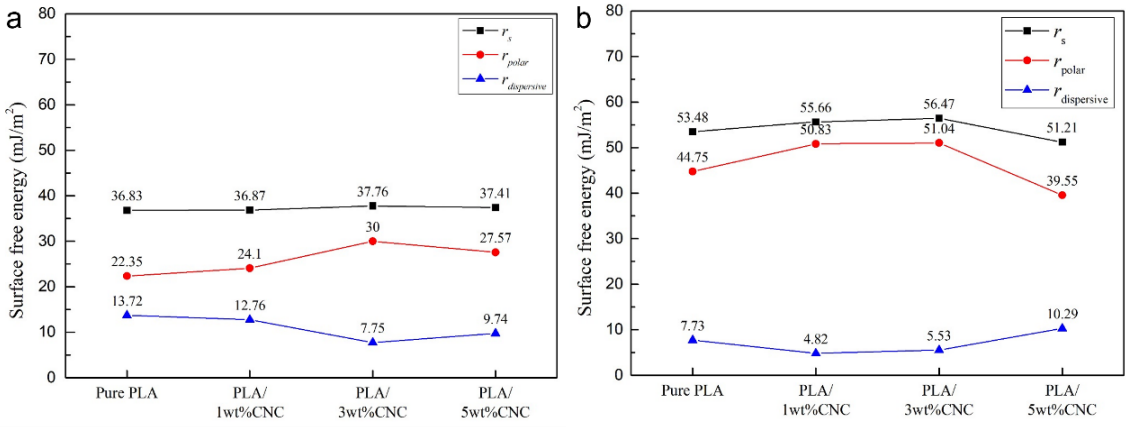

Figure. 4 Surface free energy (a) before and (b) after plasma treatment

Subsequently, after surface treatment with plasma, the average contact angle of each content decreases by approximately 20%, as shown in Figure 4a. The polar and non-polar surface free energy results are listed in Tables 7 (For pure PLA surfaces after atmospheric plasma), Table 8

(For PLA/1 wt.% CNC surfaces after atmospheric plasma modification), Table 9 (For PLA/3 wt.% CNC surfaces after atmospheric plasma modification), and Table 10 (For PLA/5 wt.% CNC surfaces after atmospheric plasma modification). The comparison of the changes in surface free energy is shown in Figure 4b. After plasma treatment, the surface free energy of each content increases on average to 54.2 mJ/m^2. The results at 3 wt.% CNC shows that the surface free energy after plasma treatment is the highest, indicating that the polar interaction force γp of 3 wt.% CNC performs the best among the overall data.

Table 3. Contact angles and surface free energy of pure PLA surfaces before plasma modification

PLA	θ_{water}	$\theta_{Glycerol}$	Surface free energy (mJ/m^2)		
			γ_s	γ_{polar}	$\gamma_{dispersive}$
A	68.58	62.04	34.75	19.14	15.61
'	69.33	66.63	33.33	23.86	9.46
B	71.60	66.56	31.84	19.20	12.64
'	72.61	66.54	31.48	17.27	14.21
C	77.26	66.04	32.85	9.287	23.56
'	74.70	67.94	45.09	43.36	1.73
D	68.71	63.33	34.19	13.64	20.55
'	62.57	68.48	45.09	43.36	1.73
E	76.79	63.07	36.77	7.38	29.38
'	76.41	63.70	35.44	27.07	8.36
Average surface free energy			**36.83**	**22.35**	**13.72**

Table 4. Surface free energy of PLA/1 wt.% CNC surfaces before plasma modification

1 wt.%CNC	θ_{water}	$\theta_{Glycerol}$	Surface free energy (mJ/m^2)		
			γ_s	γ_{polar}	$\gamma_{dispersive}$
A	61.0	59.46	40.40	9.165	31.23
'	74.87	67.56	30.55	14.51	16.04
B	70.91	67.56	32.06	21.92	10.15
'	69.43	66.88	33.25	24.02	9.23
C	63.70	62.55	38.25	30.0	8.25
'	67.41	65.65	35.01	26.53	8.48
D	69.93	62.33	34.34	17.02	17.31
'	58.62	60.24	43.93	38.10	5.82
E	69.24	61.3	35.07	17.04	18.03
'	59.46	63.95	45.84	42.76	3.08
Average surface free energy			**36.87**	**24.1**	**12.76**

Table 5. Surface free energy of PLA/3 wt.% CNC surfaces before plasma modification

3 wt.%CNC	θ_{water}	$\theta_{Glycerol}$	Surface free energy (mJ/m^2)		
			γ_s	γ_{polar}	$\gamma_{dispersive}$
A	72.37	68.42	30.98	20.17	10.81
'	70.34	63.76	33.44	18.01	15.43
B	71.42	67.60	31.70	20.94	10.76
'	70.59	67.74	32.31	22.83	9.47
C	67.54	68.78	36.20	31.27	4.93
'	63.06	67.08	42.36	39.35	3.0
D	57.03	65.06	52.65	51.53	1.12
'	63.31	66.03	40.88	36.80	4.07
E	69.50	62.75	34.16	18.31	15.85
'	63.92	69.08	43.0	40.93	2.06
Average surface free energy			**37.76**	**30.0**	**7.75**

Table 6. Surface free energy of PLA/5 wt.% CNC surfaces before plasma modification

5 wt.%CNC	θ_{water}	$\theta_{Glycerol}$	Surface free energy (mJ/m^2)		
			γ_s	γ_{polar}	$\gamma_{dispersive}$
A	78.2	72.2	27.3	14.0	13.2
'	69.3	75.4	39.9	38.9	1.01
B	60.6	69.0	50.5	49.8	0.67
'	76.9	70.3	28.5	14.1	14.4
C	69.6	74.9	38.5	37.0	1.41
'	71.3	72.0	32.6	5.04	27.6
D	76.7	70.1	28.7	14.3	14.3
'	76.2	66.2	32.0	10.9	21.0
E	72.7	74.6	32.3	27.7	3.63
'	77.0	76.8	27.7	22.6	5.1
Average surface free energy			**37.4**	**27.5**	**9.7**

Table 7. Contact angles and surface free energy of pure PLA surfaces after atmospheric plasma modification

PLA	θ_{water}	$\theta_{Glycerol}$	Surface free energy (mJ/m^2)		
			γ_s	γ_{polar}	$\gamma_{dispersive}$
A	43.8	40.8	54.1	41.1	13.0
'	50.9	61.2	60.8	60.1	0.7
B	53.3	49.8	46.4	33.5	12.9
'	49.3	50.2	51.2	43.2	7.9
C	52.4	51.7	47.8	38.4	9.3
'	49.5	53.4	53.2	48.3	4.9
D	49.9	57.9	57.8	55.9	1.8
'	49.8	47.9	49.5	38.4	11.1
E	47.4	50.2	53.8	47.4	6.3
'	50.3	50.2	59.8	40.8	8.9
Average surface free energy			**53.4**	**44.7**	**7.7**

Table 8. Surface free energy of PLA/1 wt.% CNC surfaces after atmospheric plasma modification

1wt%CNC	θ_{water}	$\theta_{Glycerol}$	Surface free energy (mJ/m^2)		
			γ_s	γ_{polar}	$\gamma_{dispersive}$
A	45.6	51.1	57.6	53.3	4.3
'	48.8	51.3	52.6	46.2	6.3
B	43.8	52.2	62.4	59.9	2.4
'	50.4	51.1	50.1	42.1	8.0
C	48.8	60.1	64.0	63.5	0.5
'	45.0	50.3	58.0	53.5	4.4
D	42.6	46.8	58.6	52.7	5.8
'	48.4	49.9	52.2	44.8	7.4
E	52.8	52.8	47.8	39.3	8.4
'	60.3	70.0	53.1	52.8	0.2
Average surface free energy			**55.6**	**50.8**	**4.82**

Table 9. Surface free energy of PLA/3 wt.% CNC surfaces after atmospheric plasma modification

3wt%CNC	θ_{water}	$\theta_{Glycerol}$	Surface free energy (mJ/m^2)		
			γ_s	γ_{polar}	$\gamma_{dispersive}$
A	43.6	52.4	63.1	60.9	2.2
'	48.3	57.8	61.2	60.0	1.2
B	48.0	48.5	52.0	43.4	8.5
'	48.9	57.4	59.0	57.4	1.7
C	55.5	45.7	46.2	23.9	22.2
'	52.0	61.0	56.7	56.7	1.1
D	49.7	58.1	58.4	56.6	1.7
'	47.9	53.7	56.2	52.5	3.6
E	49.7	48.8	49.9	40.0	9.9
'	44.3	52.2	61.4	58.7	2.7
Average surface free energy			**56.4**	**51.0**	**5.5**

Table 10. Surface free energy of PLA/5 wt.% CNC surfaces after atmospheric plasma modification

5wt%CNC	θ_{water}	$\theta_{Glycerol}$	Surface free energy (mJ/m^2)		
			γ_s	γ_{polar}	$\gamma_{dispersive}$
A	51.9	60.1	56.7	55.1	1.5
’	49.5	54.6	54.3	50.4	3.9
B	49.9	43.2	49.3	31.8	17.5
’	54.0	53.9	46.8	38.4	8.3
C	49.9	54.5	53.6	49.2	4.3
’	48.1	53.9	56.2	52.6	3.6
D	50.2	50.9	50.3	42.3	7.9
’	51.9	47.5	47.5	33.4	14.1
E	52.3	47.2	47.2	32.0	1.51
’	52.6	55.3	49.7	44.2	5.58
Average surface free energy			**51.2**	**39.5**	**10.2**

4. Conclusion

Following atmospheric plasma treatment, the surface roughness of both pure PLA and PLA/CNC composites decreases by 62% to 75%. This reduction enhances wetting properties, with optimal effects observed in the PLA/3 wt.% CNC content consistent with the hypothesis. In future composite material processing requiring adhesive bonding of PLA matrix biodegradable composites, surface plasma treatment proves efficient and convenient for rapidly enhancing wettability. However, this research is not without its limitations. The long-term durability of these plasma-treated surfaces has not been assessed, posing questions about their stability and performance over time. The experimental scale was relatively small, and scaling up the process for industrial applications could introduce challenges, including maintaining treatment uniformity and cost-effectiveness. Additionally, the focus on specific materials (PLA and PLA/CNC composites) may limit the applicability of our findings to other biodegradable polymers, which could respond differently to similar treatments. Environmental impacts of the plasma treatment process itself, such as energy consumption and emissions, were also not evaluated, which is crucial for a holistic assessment of the technology's sustainability. Lastly, the absence of comparisons with other surface modification techniques leaves room for further research to determine the most effective methods for enhancing the properties of biodegradable composites.

Author contribution

Shih-Chen Shi: Conceptualization, Methodology, Resources, Writing- Reviewing and Editing, Supervision, Project administration, Funding acquisition. Chia-Feng Hsieh: Validation, Formal analysis, Investigation, Data Curation, Writing- Original draft. Dieter Rahmadiawan: Writing-Reviewing and Editing

Funding statement

This work was supported by the National Science and Technology Council, Taiwan (grant number 111-2221-E-006-147-MY2, 111-2221-E-006-145, and 111-2221-E-006-133, 112-2221-E-006 -173). The authors gratefully acknowledge using EM000700 equipment belonging to the Core Facility Center of National Cheng Kung University.

Acknowledgments

The authors gratefully acknowledge the Core Facility Center of National Cheng Kung University. This research was partly supported by the Higher Education Sprout Project, Ministry of Education to the Headquarters of University Advancement at National Cheng Kung University (NCKU).

Conflict of interest

The authors declare that they have no known competing financial interests or personal relationships that could have appeared to influence the work reported in this paper.

References

Agrawal, C. M., & Ray, R. B. (2001). Biodegradable polymeric scaffolds for musculoskeletal tissue engineering. *Journal of Biomedical Materials Research*, *55*(2). https://doi.org/10.1002/1097-4636(200105)55:2<141::AID-JBM1000>3.0.CO;2-J

Akbar, I. M., Fauza, A. N., Abadi, Z., & Rahmadiawan, D. (2024). Study of the effective fraction of areca nut husk fibre composites based on mechanical properties. *Journal of Engineering Researcher and Lecturer*, *3*(1), 19–34. https://doi.org/10.58712/jerel.v3i1.126

Chou, C.-T., Shi, S.-C., & Chen, C.-K. (2021). Sandwich-Structured, Hydrophobic, Nanocellulose-Reinforced Polyvinyl Alcohol as an Alternative Straw Material. *Polymers*, *13*(24), 4447. https://doi.org/10.3390/polym13244447

Chou, C.-T., Shi, S.-C., Chen, T.-H., & Chen, C.-K. (2023). Nanocellulose-reinforced, multilayered poly(vinyl alcohol)-based hydrophobic composites as an alternative sealing film. *Science Progress*, *106*(1), 003685042311571. https://doi.org/10.1177/00368504231157142

Jordá-Vilaplana, A., Sánchez-Nácher, L., Fombuena, V., García-García, D., & Carbonell-Verdú, A. (2015). Improvement of mechanical properties of polylactic acid adhesion joints with bio-based adhesives by using air atmospheric plasma treatment. *Journal of Applied Polymer Science*, *132*(32). https://doi.org/10.1002/app.42391

Koizhanova, A., Magomedov, D., Abdyldayev, N., Yerdenova, M., & Bakrayeva, A. (2023). The effect of biochemical oxidation on the hydrometallurgical production of copper. *Teknomekanik*, *6*(1), 12–20. https://doi.org/10.24036/teknomekanik.v6i1.16072

Makruf, Z. I., Afnison, W., & Rahim, B. (2024). A Study on the utilization of areca nut husk fiber as a natural fibre reinforcement in composite applications: A systematic literature review. *Journal of Engineering Researcher and Lecturer*, *3*(1), 18–28. https://doi.org/10.58712/jerel.v3i1.123

Nurdin, H., Waskito, W., Fauza, A. N., Siregar, B. M., & Kenzhaliyev, B. K. (2023). The investigation of physical dan mechanical properties of Nipah-based particle board. *Teknomekanik*, *6*(2), 94–102. https://doi.org/10.24036/teknomekanik.v6i2.25972

Oktaviani, A., Zulfia, A., & Rahmadiawan, D. (2023). Enhancing laminate composites: Investigating the impact of kevlar layering and titanium carbide nanoparticles. *Teknomekanik*, *6*(2), 82–93. https://doi.org/10.24036/teknomekanik.v6i2.26572

Plastics in the Ocean - Ocean Conservancy. (n.d.). Retrieved May 26, 2024, from https://oceanconservancy.org/trash-free-seas/plastics-in-the-ocean/

Prolongo, S. G., Gude, M. R., Del Rosario, G., & Ureña, A. (2010). Surface pretreatments for composite joints: Study of surface profile by SEM image analysis. *Journal of Adhesion Science and Technology*, *24*(11–12). https://doi.org/10.1163/016942410X507623

Rahmadiawan, D., Abral, H., Ilham, M. K., Puspitasari, P., Nabawi, R. A., Shi, S.-C., Sugiarti, E., Muslimin, A. N., Chandra, D., Ilyas, R. A., & Zainul, R. (2023). Enhanced UV blocking, tensile and thermal properties of bendable TEMPO-oxidized bacterial cellulose powder-based films immersed in PVA/Uncaria gambir/ZnO solution. *Journal of Materials Research and Technology*, *26*, 5566–5575. https://doi.org/10.1016/j.jmrt.2023.08.267

Rahmadiawan, D., Abral, H., Shi, S.-C., Huang, T.-T., Zainul, R., Ambiyar, A., & Nurdin, H. (2023). Tribological Properties of Polyvinyl Alcohol/Uncaria Gambir Extract Composite as Potential Green Protective Film. *Tribology in Industry*, *45*(1), 367–274. https://doi.org/10.24874/TI.1482.05.23.06

Rahmadiawan, D., & Shi, S.-C. (2024). Enhanced Stability, Superior Anti-Corrosive, and Tribological Performance of Al2O3 Water-based Nanofluid Lubricants with Tannic Acid and Carboxymethyl Cellulose over SDBS as Surfactant. *Scientific Reports*, *14*(1), 9217. https://doi.org/10.1038/s41598-024-59010-w

Rahmadiawan, D., Shi, S.-C., Abral, H., Ilham, M. K., Sugiarti, E., Muslimin, A. N., Ilyas, R. A., Lapisa, R., & Putra, N. S. D. (2024). Comparative Analysis of the Influence of Different Preparation Methods on the Properties of TEMPO-Oxidized Bacterial Cellulose Powder Films. *Journal of Natural Fibers*, *21*(1). https://doi.org/10.1080/15440478.2023.2301386

Shi, S.-C., & Chang, Y.-W. (2022). Biofriendly chitosan-based high-efficiency dialysis membrane. *Progress in Organic Coatings*, *170*, 106981. https://doi.org/10.1016/j.porgcoat.2022.106981

Shi, S.-C., Chen, T.-H., & Mandal, P. K. (2020). Enhancing the Mechanical and Tribological Properties of Cellulose Nanocomposites with Aluminum Nanoadditives. *Polymers*, *12*(6), 1246. https://doi.org/10.3390/polym12061246

Shi, S.-C., & Chen, X.-A. (2023). Cellulose circular economy: Amino-functionalized graphene quantum dots as highly sensitive vaccine indicators. *Industrial Crops and Products*, *206*, 117694. https://doi.org/10.1016/j.indcrop.2023.117694

Shi, S.-C., & Huang, T.-F. (2018). Effects of temperature and humidity on self-healing behaviour of biopolymer hydroxylpropyl methylcellulose for ecotribology. *Surface and Coatings Technology*, *350*, 997–1002. https://doi.org/10.1016/j.surfcoat.2018.03.039

Shi, S.-C., Lu, F.-I., Wang, C.-Y., Chen, Y.-T., Tee, K.-W., Lin, R.-C., Tsai, H.-L., & Rahmadiawan, D. (2024). Rice straw-derived chitosan-enhanced plasticizers as biologically and environmentally friendly alternatives for sustainable materials. *International Journal of Biological Macromolecules*, *264*, 130547. https://doi.org/10.1016/j.ijbiomac.2024.130547

Shi, S.-C., Ouyang, S.-W., & Rahmadiawan, D. (2024). Erythrosine–Dialdehyde Cellulose Nanocrystal Coatings for Antibacterial Paper Packaging. *Polymers*, *16*(7), 960. https://doi.org/10.3390/polym16070960

Shi, S.-C., & Tsai, X.-N. (2022). Cellulose derivative as protection coating: Effect of nanoparticle additives on load capacity. *Teknomekanik*, *5*(2), 90–96. https://doi.org/10.24036/teknomekanik.v5i2.16372

Shi, S.-C., Tsai, X.-N., & Rahmadiawan, D. (2024). Enhancing the tribological performance of hydroxypropyl methylcellulose composite coatings through nano-sized metal and oxide additives: A comparative study. *Surface and Coatings Technology*, *483*, 130712. https://doi.org/10.1016/j.surfcoat.2024.130712

Shi, S.-C., & Wu, J.-Y. (2018). Deagglomeration and tribological properties of MoS2/hydroxypropyl methylcellulose composite thin film. *Surface and Coatings Technology*, *350*, 1045–1049. https://doi.org/10.1016/j.surfcoat.2018.02.067